

Investigation of Restricted Diffusion Behaviour of Intramyocellular Lipids in Skeletal Muscle

Peng Cao^{1,2}, Zhongwei Qiao^{1,2}, Anna M. Wang^{1,2}, Shujuan Fan^{1,2}, Victor B. Xie^{1,2}, Jian Yang^{1,3}, and Ed X. Wu^{1,2}

¹Laboratory of Biomedical Imaging and Signal Processing, The University of Hong Kong, Hong Kong SAR, China, People's Republic of, ²Department of Electrical and Electronic Engineering, The University of Hong Kong, Hong Kong SAR, China, People's Republic of, ³Medical Imaging Center of the First Affiliated Hospital, School of Medicine of Xi'an Jiaotong University, Xi'an, Shanxi Province, China, People's Republic of

INTRODUCTION: In skeletal muscle, lipids are stored as intramyocellular lipid (IMCL) inside muscle cells and extramyocellular lipid (EMCL) in large adipocytes (1). IMCL serves as the principal reservoir for storing cellular energy. It exists in form of small spherical droplets that are often found next to mitochondria. IMCL droplet is composed of a relatively homogeneous lipid ester core and a phospholipid monolayer (2), thus presenting a highly restricted environment for lipid diffusion. In vivo MR characterization of such IMCL diffusion may provide insights into the dynamic balance between lipid droplet synthesis and degradation in lipid metabolism. Recently, severely hindered IMCL diffusion has been reported experimentally in a human 3T study using diffusion-weighted MRS (DW-MRS). However, the IMCL diffusion could not be measured in this study due to the technical challenges associated with the high b-value requirement and vulnerability to motion and gradient eddy current (3). More recently, the apparent diffusion coefficient (ADC) of IMCL has been determined for rat skeletal muscle in vivo with diffusion time $\Delta=90\text{ms}$ (4). In this study, we hypothesized that DW-MRS could probe the IMCL diffusion restricted within the droplet microstructure. Specifically, we aimed to investigate the effect of diffusion time Δ on IMCL ADC and EMCL ADC in normal rat hindlimb muscles in vivo.

MATERIALS AND METHODS: **Animal Preparation:** Normal adult male Sprague-Dawley (SD) rats (N=6; 2-month old, 420-450g) were studied by DW-MRS under normal feeding condition. During the MR experiments, animals were anesthetized with a mixture of air and 1-1.5% isoflurane, fixed by an in-house hindlimb fixation device, and mechanically ventilated. Muscle paralyzer (Pavulon; 1mg/kg IP) was also administered to further reduce the small physiological motions such as muscle tone related motion. **MRI Protocol:** All MRI measurements were made using a 7T Bruker scanner equipped with a 370mT/m gradient system along each axis. The pre-emphasis of gradient system was carefully adjusted, exhibiting minimum eddy current along x axis. For DW-MRS, a stimulated-echo (STEAM) based single-voxel MRS sequence was implemented by adding a pair of unipolar diffusion gradients along the x axis during the two TE/2 intervals. To further reduce any potential eddy current influence, the gradient off period between the second diffusion gradient and readout was prolonged to be 8.12ms. DW spectra were acquired with diffusion duration $\delta=30\text{ms}$, 7 b-values (0 to $3.03 \times 10^5 \text{ s/mm}^2$) along x axis, 2 diffusion times ($\Delta = 80$ and 220ms), TR/TE=1500/80ms, spectral width=4kHz, water suppression, NEX=64, and voxel size= $8 \times 8 \times 8\text{mm}^3$. Note that such a STEAM based sequence is advantageous over the PRESS based DW-MRS sequence (used in previous study (4)) because it offers the flexibility to increase diffusion time while the lipid SNR remains largely preserved. All MR experiments were performed on the lower rat hindlimbs. Prior to DW-MRS acquisition, T1-weighted 2D RARE imaging was employed to facilitate voxel localization in a reproducible manner (Fig. 1a). **Data Analysis:** Spectral analysis was performed using the JMRUI and Bruker TOPSPIN software package. IMCL (i-CH₂) and EMCL (e-CH₂) signals were quantified by fitting the spectrum to a Gaussian line shape using the AMARES algorithm in JMRUI software. The quantification was considered to be relevant only when the corresponding Cramer-Rao lower bounds were below 25%. ADCs of IMCL and EMCL were calculated by fitting their b-value-dependent signals to a monoexponential model. All measurements were expressed as mean \pm standard deviation. Two-tailed unpaired student's t-test was employed to examine the ADC difference between two diffusion times. To examine the IMCL droplet microstructure, excised muscle samples were prepared from normal rat hindlimb muscles and analyzed using Oil Red O immunohistochemical staining (5).

RESULTS AND DISCUSSIONS: Diffusion decays were observed to be approximately monoexponential for both IMCL (i-CH₂) and EMCL (e-CH₂) with the b-value range studied (Figs. 1b and 1c). When diffusion time Δ increased from 80ms to 220ms, IMCL ADC exhibited significant decrease, i.e., from $(2.26 \pm 0.63) \times 10^{-6} \text{ mm}^2/\text{s}$ to $(1.55 \pm 0.39) \times 10^{-6} \text{ mm}^2/\text{s}$ (Fig. 1 and Fig. 2). Such diffusion time dependence indicated the spatially restricted IMCL diffusion. Meanwhile, EMCL ADCs were higher than IMCL ADCs, and they showed insignificant change, i.e., $(1.36 \pm 0.23) \times 10^{-5} \text{ mm}^2/\text{s}$ vs. $(1.29 \pm 0.20) \times 10^{-5} \text{ mm}^2/\text{s}$ for $\Delta=80\text{ms}$ and $\Delta=220\text{ms}$ (Fig. 2). Histological analysis revealed that the IMCL droplets from normal rat hindlimb muscle samples had diameters typically equal or less than $2\mu\text{m}$, and were scattered in cytoplasm of muscle cells (Fig. 3). Also note that IMCL droplets were preferentially scattered or distributed within certain muscle cells or types (i.e., oxidative types), in consistency with earlier histological reports (5). Given that the lipid forms are similar in IMCL and EMCL (i.e., triglycerides), we assume that unrestricted lipid diffusion coefficient can be reasonably approximated by the EMCL ADC. Thus the average diffusion distance experienced by free lipid macromolecule can be estimated as $\sqrt{2D\Delta} = 1.47\mu\text{m}$ at $\Delta=80\text{ms}$ and $\sqrt{2D\Delta} = 2.38\mu\text{m}$ at $\Delta=220\text{ms}$. These two diffusion distances were comparable to the IMCL droplet dimension ($2\mu\text{m}$ or less in diameter) observed in Fig. 3. Therefore, the small spherical microstructure of IMCL droplets is mostly likely responsible for the decreased lipid ADC in IMCL (as compared to EMCL ADC), and the decrease of IMCL ADC with diffusion time Δ as observed in this study.

CONCLUSION: Our experimental results demonstrated that the small IMCL microstructure leads to highly restricted lipid diffusion in IMCL droplet. Such MR determination of IMCL diffusion characteristics may provide a sensitive maker to probe the IMCL droplet microstructure, leading to a potentially valuable tool for investigating IMCL droplet dynamics and metabolism in vivo.

REFERENCES: 1. Howald H, et al. J Appl Physiol 2002;92:2264-72; 2. Martin S, et al. Nat Rev Mol Cell Biol 2006;7:373-8; 3. Brandejsky V, et al. Magn Reson Med 2011; 4. Xiao L, et al. Magn Reson Med 2011;66:937-44; 5. Spangenburg EE, et al. J Biomed Biotechnol 2011;2011:598358.

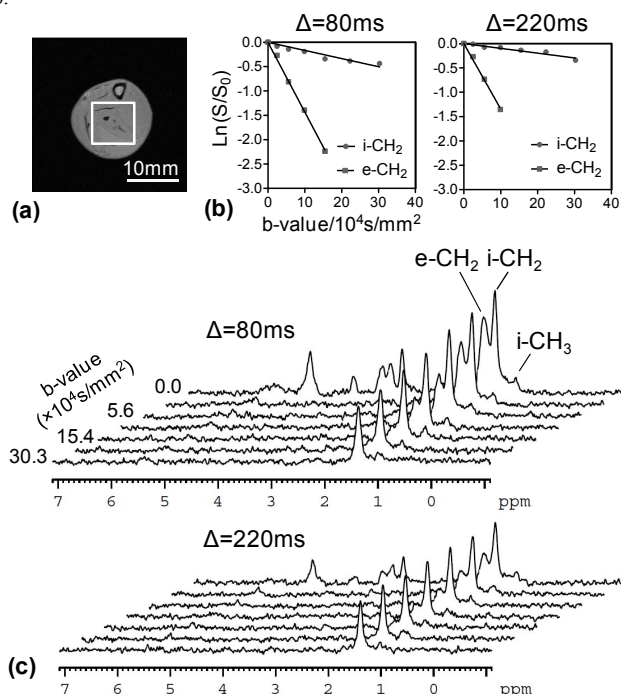


Fig. 1: In vivo MR diffusion characteristics of IMCL (i-CH₂) and EMCL (e-CH₂) observed in the lower hindlimb muscle of a normal adult SD rat. (a) Axial MR image showing the MRS $8 \times 8 \times 8\text{mm}^3$ voxel. (b) Diffusion decays at diffusion time Δ of 80ms and 220ms. (c) DW spectra at various b-values with two diffusion times. Note the slower diffusion decay with longer diffusion time in (c).

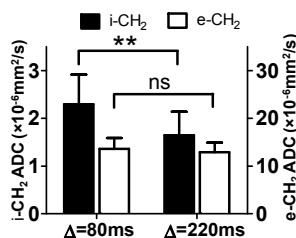


Fig. 2: IMCL (i-CH₂) and EMCL (e-CH₂) ADC vs. diffusion time Δ . ** for $p < 0.01$ and ns for not significant.

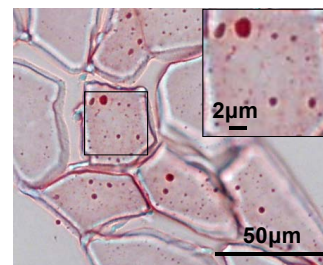


Fig. 3: Oil Red O staining of IMCL droplets in normal rat hindlimb muscle. They are marked by the red dots/spheres scattered mostly inside the cytoplasm of certain muscle cells, with diameters typically less than $2\mu\text{m}$.